EFFECT OF COOLING AIR ON SWIRL COMBUSTOR

Showkat Jahan Chowdhury and Md. Shiblee Noman
Mechanical Engineering Department, Alabama A&M University
P.O. Box 1163, Huntsville, AL 35762, U.S.A.
Email: s.chowdhury@email.aamu.edu, sjchowdhury931@yahoo.com

Abstract: *This paper presents the numerical study of the turbulent swirling flow in a combustor and the effect of cooling air, which has practical applications in industrial furnaces and jet engines. Cooling air is used to protect the combustor wall from burnout, while allowing the combustion to occur at higher temperature. The governing differential equations using k – ε turbulence model closure are solved by a control-volume based iterative finite difference technique. Computations are done for constant vane angle type swirl generation at inlet. Different swirl numbers up to 1.5 are considered. To study the effect of cooling air on the combustor performance, calculations are repeated for two different velocities of the cooling air jet. The predicted distribution of the mean axial and tangential velocities, turbulence kinetic energy and streamline plots are discussed in the article. With the increase of swirl strength, secondary on-axis recirculation due to swirl is observed. The swirl produces larger turbulence kinetic energy and enhances mixing rate, thus require shorter combustor length. The interaction between the non-swirling cooling air and swirling core flow also increases the generation of turbulence kinetic energy and mixing rate. The capability of the computational model for predicting recirculating flows is tested by comparing the results with available experimental data and found to have reasonable matching.*

INTRODUCTION

Turbulent swirling flow with abrupt axisymmetric expansion, as found in swirl combustors, is a complex flow possessing several distinctly different flow regimes. The purpose of adding swirl to flows entering furnace and jet engine combustors is to enhance flame stability and mixing[1,2]. The sudden expansion geometry in swirl combustors produces mixing rates downstream of the expansion that are substantially higher than those without it. The elevated mixing rates are due to very high levels of turbulence kinetic energy generated by shearing as the flow experiences radial expansion. Sufficiently strong swirl produces secondary on-axis recirculation which is driven by an adverse pressure gradient that results from the viscous dissipation of the tangential velocity component as the flow proceeds downstream. Though this recirculation contributes to mixing indirectly through convective processes, the primary enhancement in mixing is assumed to result from the rotational shear strain generating higher levels of turbulence. Any increase in shear strain tends to raise the level of transfer of mean kinetic energy to turbulence energy. Near the combustor wall where the length scales are small, dissipation dominates because the dissipation is inversely proportional to the length scale. But in the high shear regions away from the wall, length scales are large and dissipation rates consequently low. Thus, in these high-shear secondary recirculation regions away from the wall, turbulence kinetic energy generated dissipates relatively slowly, and its level found is much higher. The type of rotational motion, solid body or free vortex type also has different effects on stresses and turbulence energy. To allow higher temperature in the combustor while protecting the wall from burnout, non-swirling cooling air is admitted close to the wall. The interaction between this non-swirling cooling air jet and the core swirling flow contributes to the generation of higher levels of turbulence energy, away from the wall. Hence, an in-depth knowledge of properties is required before manufacturing such equipment. In combustor development, designers are aided by experiments, but as a supplement to them, economical design and operation can be greatly facilitated by the availability of prior properties of the flow-field through some computational model.

The objective of the present study is to obtain numerical predictions for the flow in the swirl combustor with cooling air for various swirl strength, and to analyze the effect of the cooling air by changing its velocity relative to the core flow. Though sophisticated turbulence models have been developed, yet the k – ε model is still widely used in the industry due to its simplicity and as it has already been accommodated into many commercially available computer codes. Hence, in the present study the k – ε model[3] is used.

NOMENCLATURE

C_1, C_2, C_μ	:coefficients in turbulence model
k	:turbulent kinetic energy
r	:radial coordinate
R_1	:radius of the hub of the swirl generator
R_2	:radius of the tip of the swirl generator
R	:radius of the combustor duct
Re	:Reynolds number
S	:Swirl number
S_φ	:source term for variable φ
u	:mean axial velocity
U_o	:reference velocity
v	:mean radial velocity
w	:mean tangential velocity
x	:axial coordinate
Γ	:diffusivity
ε	:dissipation rate of turbulence kinetic energy
μ	:dynamic viscosity
θ	:swirl vane angle
ρ	:constant mass density
σ_φ	:Prandtl number for variable φ

Table 1. Source terms for the General Eq. (1).

φ Value	Name of Equation	Source Term (S_φ)
1	Continuity	0
u	u-momentum (axial)	$-\frac{\partial p}{\partial x}+S^u$
v	v-momentum (radial)	$-\frac{\partial p}{\partial r}+\frac{\rho w^2}{r}-\frac{2\mu v}{r^2}+S^v$
w	w-momentum (tangential)	$-\frac{\rho v w}{r}-\frac{w}{r^2}\frac{\partial}{\partial r}(r\mu)$
k	k-equation	$G-C_D\rho\varepsilon$
ε	ε- equation	$\left(C_1\varepsilon G-C_2\rho\varepsilon^2\right)/k$

BASIC EQUATIONS AND NUMERICAL DETAILS

The equations governing the axisymmetric, swirling turbulent flow in cylindrical coordinates using the k – ε model closure of Launder and Spalding [3] can all be written in the common form as,

$$\frac{1}{r}\left[\frac{\partial}{\partial x}(\rho u r\varphi)+\frac{\partial}{\partial r}(\rho v r\varphi)-\frac{\partial}{\partial x}\left(r\Gamma_\varphi\frac{\partial\varphi}{\partial x}\right)-\frac{\partial}{\partial r}\left(r\Gamma_\varphi\frac{\partial\varphi}{\partial r}\right)\right]=S_\varphi \quad (1)$$

Here, the flow is assumed to be steady and incompressible. In the above Eq. (1), the first two terms in the left hand side are the convection terms whereas the third and forth terms are the diffusion terms. The term S_φ in the right hand side is the source term which contains terms describing the generation and consumption of variable φ. The forms for the source term S_φ are given in Table 1, where

$$S^u=\frac{1}{r}\frac{\partial}{\partial r}\left(r\mu\frac{\partial v}{\partial x}\right)+\frac{\partial}{\partial x}\left(\mu\frac{\partial u}{\partial x}\right) \quad (2)$$

$$S^v=\frac{\partial}{\partial x}\left(\mu\frac{\partial u}{\partial r}\right)+\frac{1}{r}\frac{\partial}{\partial r}\left(r\mu\frac{\partial v}{\partial r}\right) \quad (3)$$

$$G=\mu\left[2\left\{\left(\frac{\partial u}{\partial x}\right)^2+\left(\frac{\partial v}{\partial r}\right)^2+\left(\frac{v}{r}\right)^2\right\}+\left(\frac{\partial u}{\partial r}+\frac{\partial v}{\partial x}\right)^2+\left\{r\frac{\partial}{\partial r}\left(\frac{w}{r}\right)\right\}^2+\left(\frac{\partial w}{\partial x}\right)^2\right] \quad (4)$$

$$\mu=C_\mu\rho k^2/\varepsilon+\mu_1 \text{ and } \Gamma_\varphi=\mu/\sigma_\varphi \quad (5)$$

For continuity equation $\Gamma_\varphi = 0$, for the momentum equations $\sigma_\varphi = 1$ and the turbulence model constants are assigned the following values[3]

$$C_\mu=0.09, C_1=1.44, C_2=1.92,\ \sigma_k=1.0,\ \sigma_\varepsilon=1.3 \quad (6)$$

The computational domain for the swirl combustor is shown in Fig. 1. Two coaxial jets of axial velocity U_1 and U_2 are coming in through the swirl generator and annular space close to the combustor wall, respectively. The hub of the swirler has a radius of R_1 = 0.95 cm, and the tip has a radius of R_2 = 2.85 cm. Dilution or cooling air admitted between the outer radius of the swirler and the combustor wall is non-swirling. The velocity of the cooling air with respect to the core flow is changed to study the effect on the combustor performance. Swirl can be imparted to the inner annular jet using solid body or constant vane angle type swirl generator. For solid body rotation swirl generation, the tangential velocity *w* varies linearly with radius *r*. But for constant vane angle swirl generation, the tangential velocity *w* is calculated as *u tanθ* where *u* is the axial velocity and *θ* is the vane angle. The swirl number *S* is defined as

$$S=\int_0^R r^2u_{in}w_{in}dr\Big/R\int_0^R ru_{in}^2dr \quad (7)$$

where u_{in} and w_{in} are the velocities at inlet. The coaxial jets then experience sudden radial expansion into the combustor duct having radius *R* = 4.0 cm.

A staggered mesh finite volume method is used to discretize the differential equations written in general form as expressed in Eq. (1). The computational domain is divided by a 46 X 34 non-uniform grid with finer spacing in the regions of large spatial gradients. The above differential equations are integrated over their appropriate staggered control volumes and discretized using a hybrid differencing scheme[4]. No slip boundary conditions along with wall functions are applied at solid walls. The turbulence kinetic energy *k* and the dissipation rate ε at inlet are calculated as

$$k_{in}=\lambda_1u_{in}^2\ ;\ \varepsilon_{in}=\frac{k_{in}^{3/2}}{\lambda_2R} \quad (8)$$

where λ_1 and λ_2 are two constants having the values of 0.03 and 0.02, respectively. At the outlet boundary and symmetry axis, zero gradient conditions are applied. The discretized equations with boundary condition modifications are solved using the SIMPLE[5] and TDMA algorithm. Here, semi-implicit line-by-line relaxation method is employed to obtain converged solutions iteratively. Under relaxation factors are also used to promote computational stability.

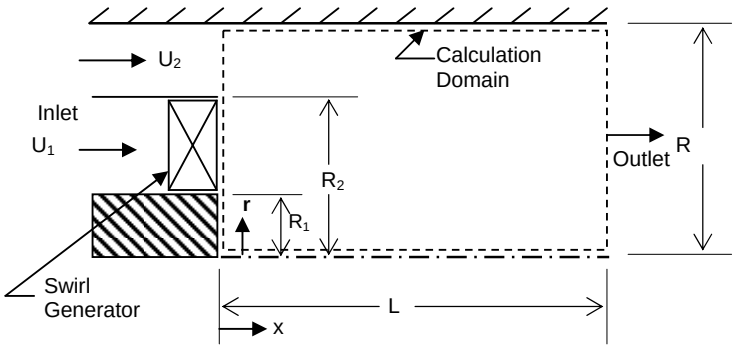

Fig. 1 Geometry of swirl combustor with cooling air.

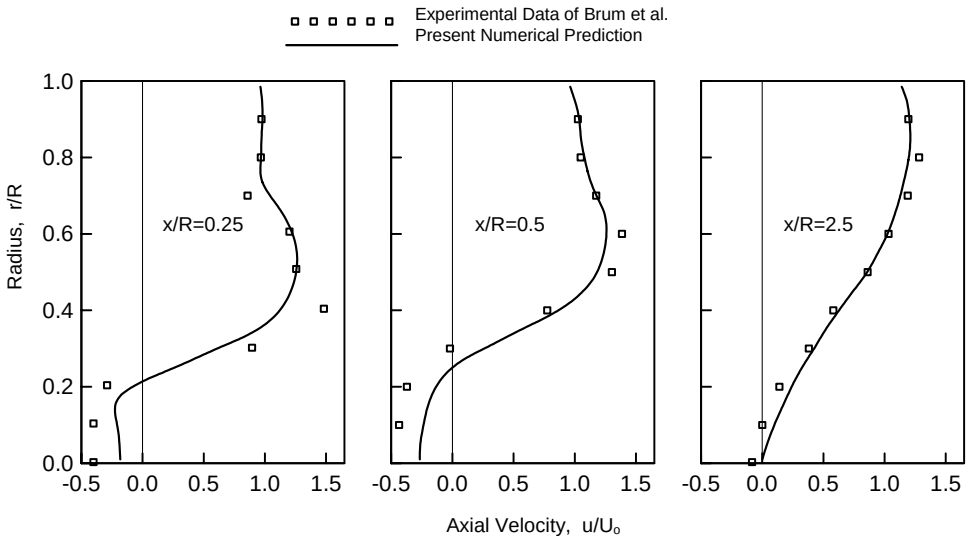

Fig. 2 Comparison of computed dimensionless mean axial velocity profiles with experimental data.

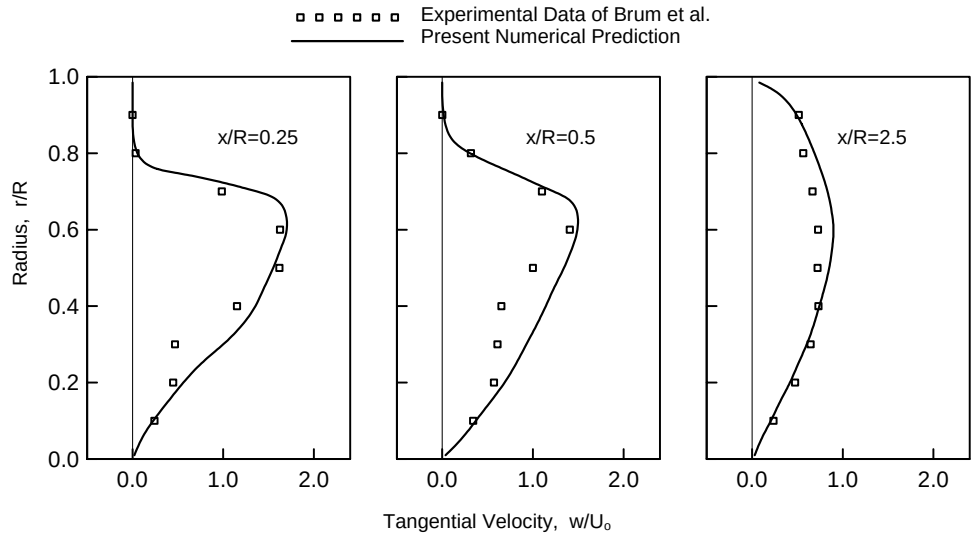

Fig. 3 Comparison of computed dimensionless mean tangential velocity profiles with experimental data.

RESULTS AND DISCUSSION

The turbulent swirling flow in the combustor with cooling air and sudden expansion, as shown in Fig. 1, is analyzed numerically using the above computational code and the results are presented below.

The non-reacting flow was also studied experimentally by Brum and Samuelsen[6] for the configuration as shown in Fig. 1. The combustor tube was 50 cm long with rectangular windows on each side to measure the axial and swirl components of velocity using forward scatter measurement techniques with a two-color laser anemometry system. The swirl was generated by a 12-vane sheet metal swirler at the inlet cross-section. In the hub of the 60^o swirler, a cone or annular nozzle (not shown here) was installed for injection of CO_2 in the non-reacting measurements. Dilution or cooling air was admitted between the outer diameter of the swirler and the duct wall. The annular flow through the swirler and the dilution air had axial velocities of 15.6 m/s and 15.4 m/s, respectively. The computational code is first used to simulate the flow for the experimental conditions of Brum and Samuelsen[6]. Inlet profiles are taken partially from available experimental data near the inlet. The injection of CO_2 which was only 1.3 % of the flow-rate is not included in the computation due to lack of data. The numerical predictions are compared with the experimental data in Fig. 2 and Fig. 3. In these figures the solid lines correspond to the computational results whereas the boxes correspond to the experimental data of Brum and Samuelsen[4]. The distribution of the mean axial velocity is compared in Fig. 2 whereas Fig. 3 compares the variation of the mean tangential velocity at different sections. Here *x* is the axial distance from the sudden expansion section at inlet and *R* is the radius of the combustor. The velocities are nondimensionalized with the aid of the reference velocity U_o, which is the average axial velocity through the swirl generator at inlet. It appears that the predictions of the present model are in good agreement with the experimental data, except for the axial velocity at x/R = 0.25,

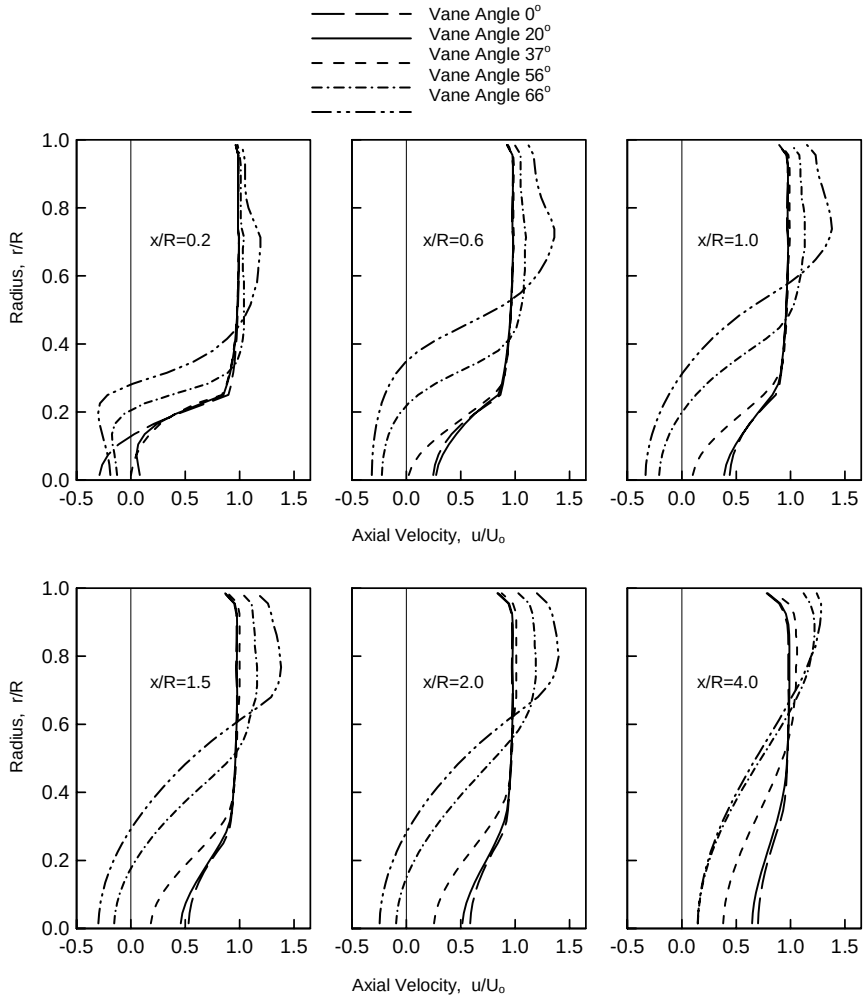

Fig. 4 Comparison of dimensionless mean axial velocity profiles due to constant vane angle swirl generator, for case I.

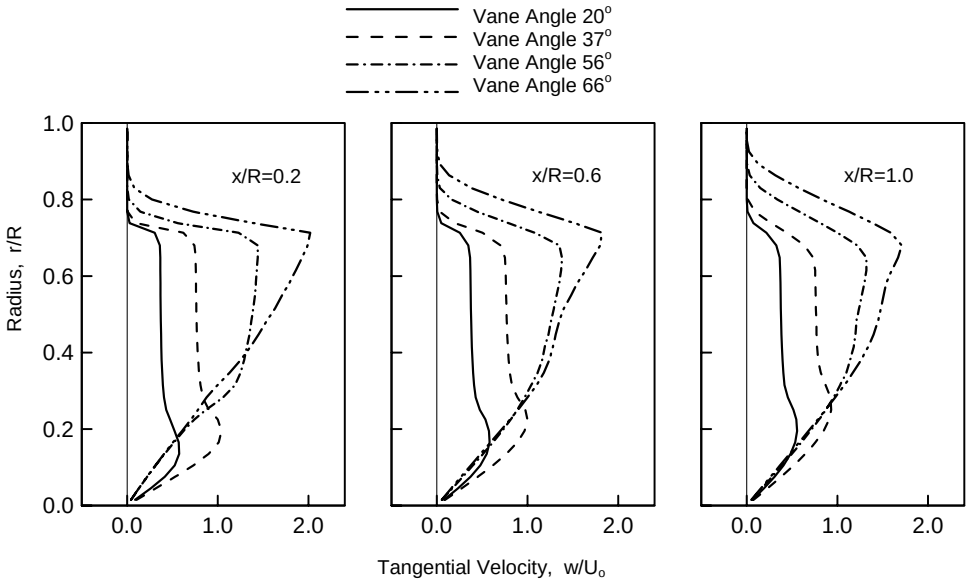

Fig. 5 Comparison of dimensionless mean tangential velocity profiles due to constant vane angle swirl generator, for case I.

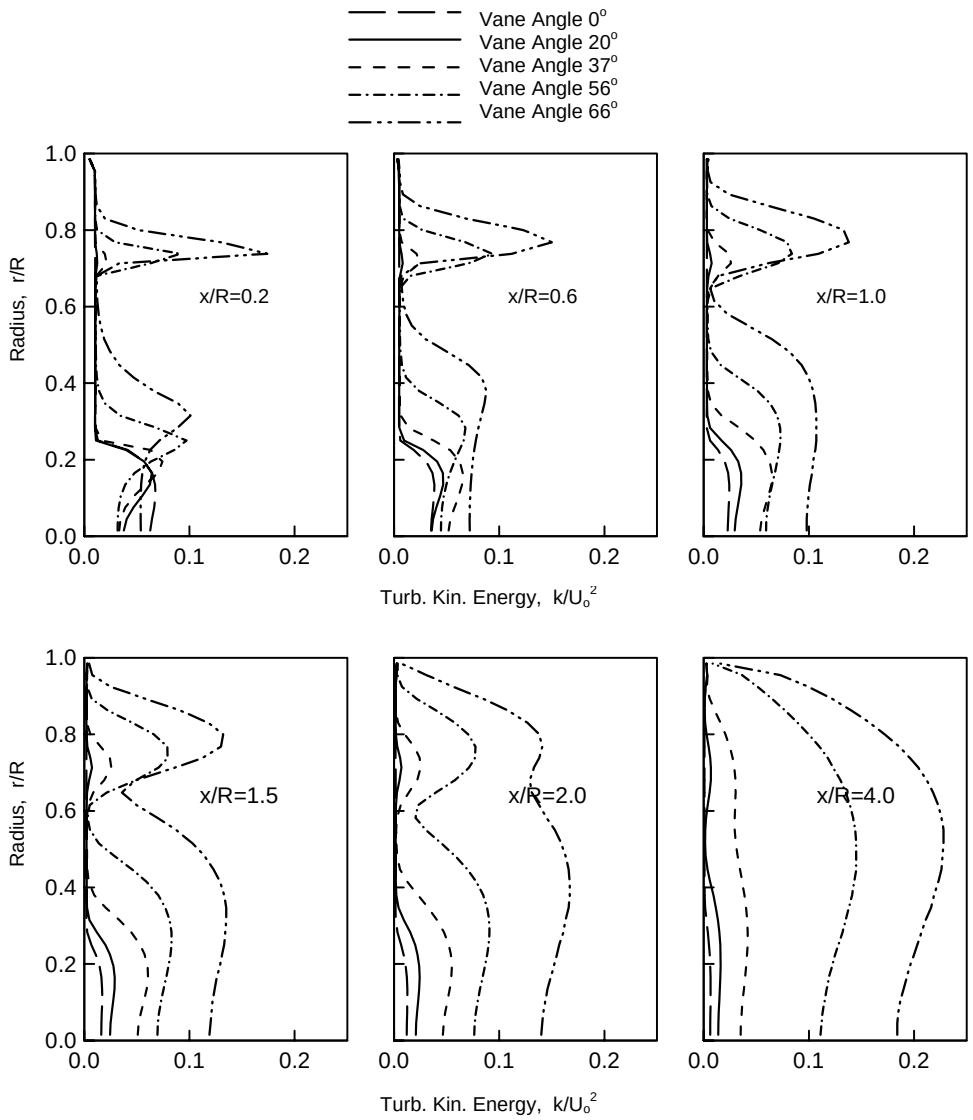

Fig. 6 Comparison of dimensionless turbulence kinetic energy profiles due to constant vane angle swirl generator, for case I.

which might be as a consequence of neglecting the CO_2 injection at inlet. Hence, it may be concluded that the present numerical model has the capability of predicting complex turbulent flows with reasonable accuracy.

It has been found earlier[7, 8] that generation of turbulence kinetic energy and hence mixing rate is better for constant vane angle swirl generation, compared to solid body rotation swirl generation at inlet. The computational model is then used to analyze the flow of Fig. 1 having constant vane angle swirl generation at inlet just before expansion for the inner annular jet, while the outer jet of cooling air is assumed to be non-swirling. Uniform inlet axial velocities for the inner and outer annular jets are taken as 15.6 m/s and 15.4 m/s, respectively at a Reynolds number of Re = 40000 based on the inner annular jet through the swirler, and is considered as Case – I. The length of the calculation domain (L) is taken as 0.5 m. Computations are done for different swirl vane angles $\theta = 0^o$, 20^o, 37^o, 56^o, and 66^o corresponding to swirl numbers S = 0, 0.25, 0.50, 1.00 and 1.50, respectively and the results are shown in Figs. 4 – 7. The flow parameters are non-dimensionalized by the reference velocity $U_o = U_1 = 15.6$ m/s.

The distribution of the predicted dimensionless mean axial velocity across the flow for the above swirl vane angles at different axial locations away from the sudden expansion geometry is shown in Fig. 4 for comparison. Here, one finds that for vane angle $\theta = 0^o$ (non-swirling flow) small primary recirculation near the centerline has developed due to sudden expansion, as can be seen by the negative *u* velocity at x/R = 0.2. But as the vane angle increases to $\theta = 20^o$ the primary recirculation vanishes. For swirl vane angles $\theta = 56^o$ and 66^o, one observes that the axial velocity near the centerline is negative and large secondary on-axis recirculation has developed. With the increase of swirl strength, the magnitude of the secondary on-axis recirculation due to swirl increases. At x/R = 4.0,

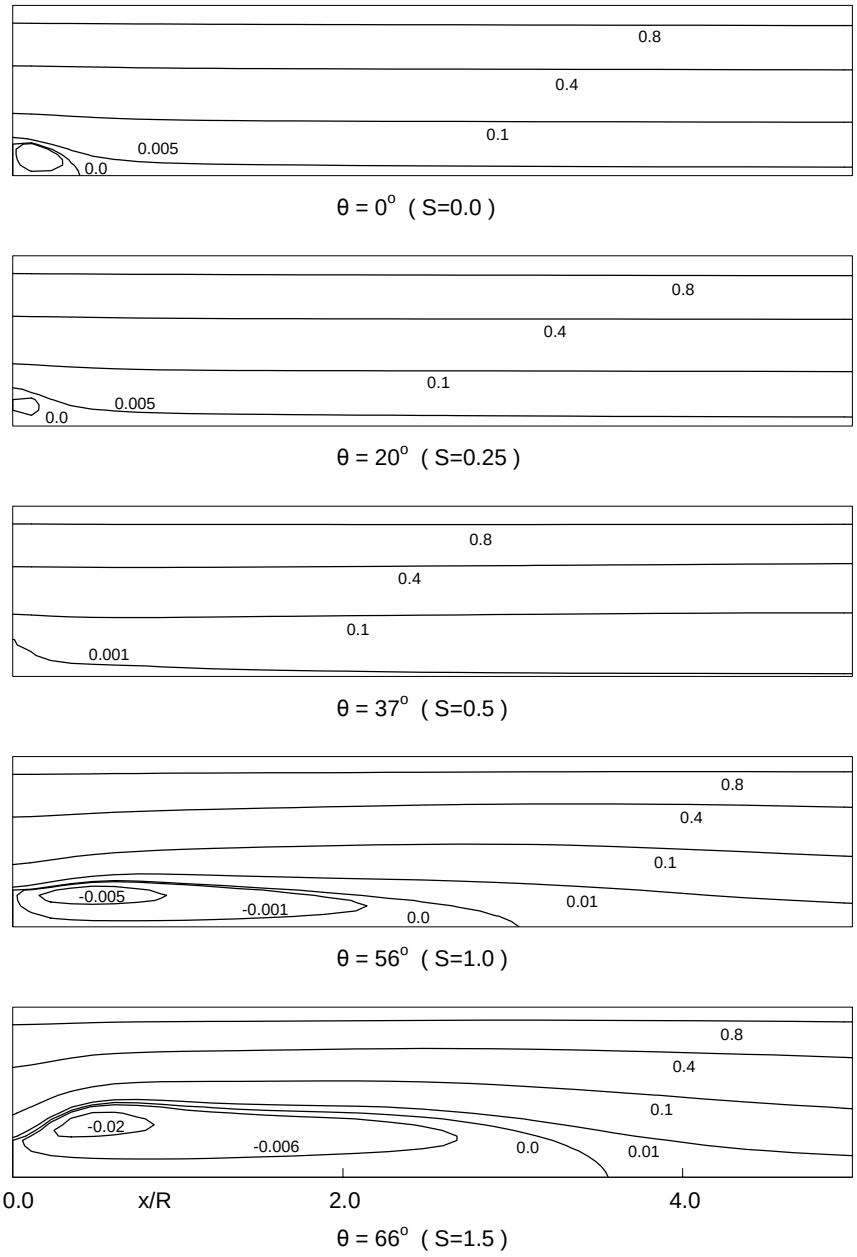

Fig. 7 Streamline plots for constant vane angle swirl generation at inlet, case I.

.

the axial velocity profiles for moderate and high swirl become similar.

Figure 5 shows the variation of the dimensionless mean tangential velocity profiles across the flow at different sections. As already mentioned, the dissipation of tangential velocity increases the pressure and produces an adverse pressure gradient along the flow which consequently produces secondary on-axis recirculation due to swirl. For $\theta = 20^o$ and 37^o (low swirl), the mean tangential velocity is not sufficient to produce the adverse pressure gradient required for secondary on-axis recirculation. But when $\theta = 56^o$ or 66^o the mean tangential velocity near the centerline decreases substantially, unlike to those for $\theta = 20^o$ and 37^o. This in turn increases the pressure and produces an adverse pressure gradient and thereby recirculation. As the dissipation of tangential velocity for $\theta = 66^o$ is more compared to that for $\theta = 56^o$, hence the size and intensity of recirculation for $\theta = 66^o$ is larger. In the region close to the combustor inlet, where the temperature in the core is very high due to combustion, the tangential velocity near the combustor wall is zero, which means that the non-swirling cooling air is maintaining a buffer zone to protect the wall.

The variations of dimensionless turbulence kinetic energy across the flow at different sections are shown in Fig. 6 for comparison. The turbulence kinetic energy produced for swirl vane angle $\theta = 56^o$ and 66^o increases with the increase

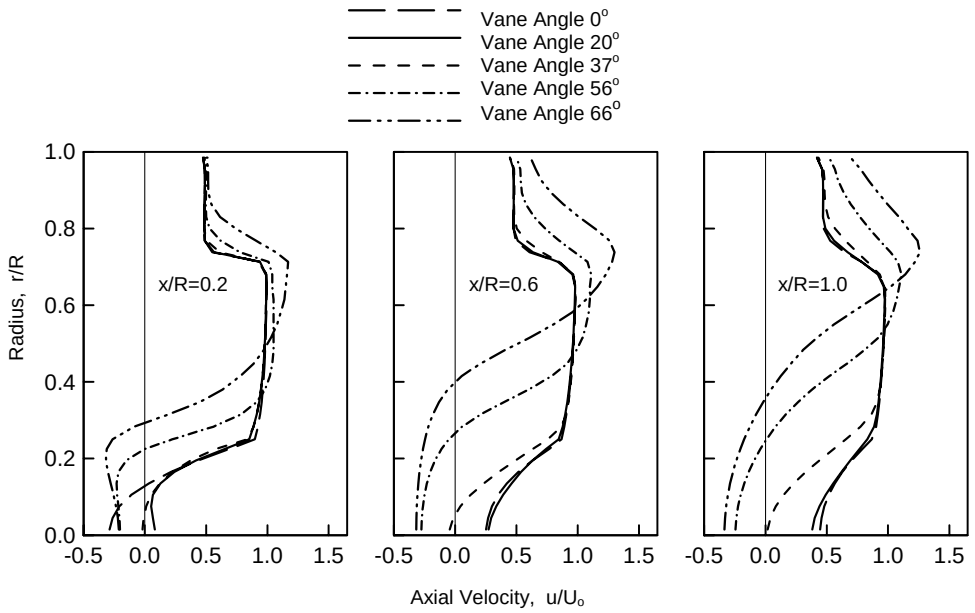

Fig. 8: Comparison of dimensionless mean axial velocity profiles due to constant vane angle swirl generator, for case II.

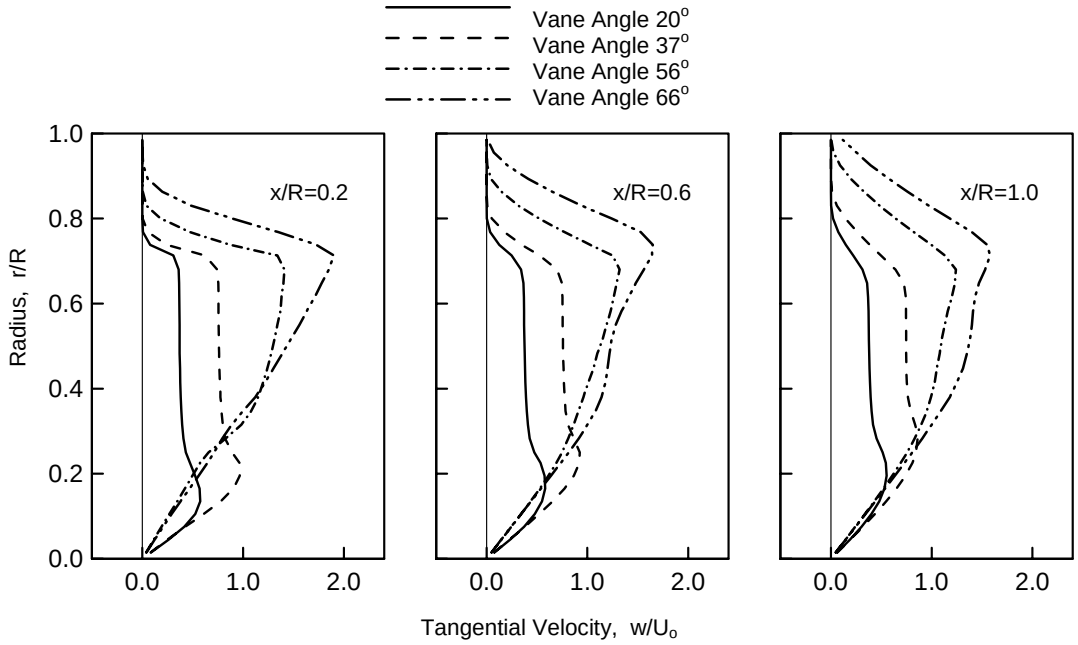

Fig. 9: Comparison of dimensionless mean tangential velocity profiles due to constant vane angle swirl generator, for case II.

of swirl strength and is found to be much larger which is desired as compared to that for $\theta = 0^o$, 20^o and even 37^o. The secondary on-axis recirculation due to swirl, and the rotational strain between the inner swirling jet and outer non-swirling cooling air produces greater turbulence kinetic energy. Also as these regions are away from the combustor wall, so dissipation rate is low. As a result, higher levels of turbulence kinetic energy is available, which enhances the mixing rate required for complete combustion in a shorter combustor length.

The streamline plots for different inlet swirl vane angles of 0^o, 20^o, 37^o, 56^o and 66^o are shown in Fig. 7. For swirl vane angle $\theta = 0^o$ (i.e. non-swirling flow), one observes only small primary recirculation due to sudden expansion. As the swirl vane angle is changed to $\theta = 20^o$ (i.e. low swirl), the length of primary recirculation zone decreases, and vanishes at $\theta = 37^o$. As the swirl vane angle is increased to $\theta = 56^o$, secondary on-axis recirculation is developed. When the swirl vane angle is further increased to

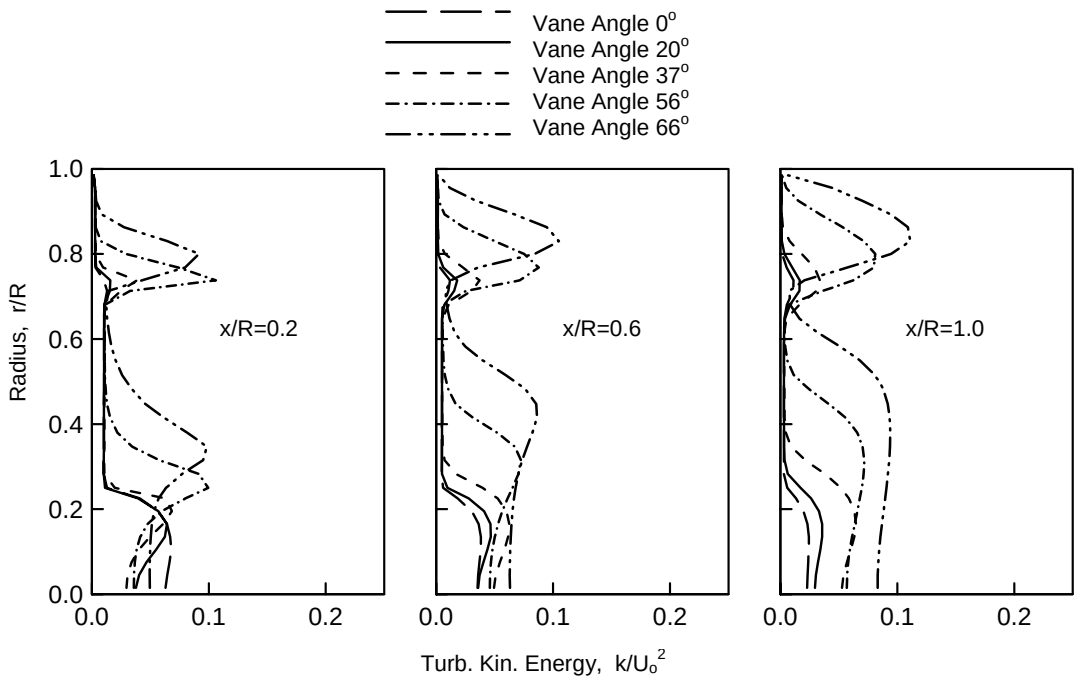

Fig. 10 Comparison of dimensionless turbulence kinetic energy profiles due toconstant vane angle swirl generator, for case II.

$\theta = 66^o$, the secondary on-axis recirculation due to swirl becomes quite large.

In order to study the effect of the cooling air, the computational model is again used to simulate the flow in Fig. 1, having constant vane angle swirl generation at inlet just before expansion for the same inner jet through the swirler, while changing the velocity of the non-swirling outer jet of cooling air. Uniform inlet axial velocities for the inner and outer annular jets are taken as 15.6 m/s and 7.7 m/s, respectively at a Reynolds number of Re = 40000 based on the inner annular jet through the swirler, and is considered as Case – II. The length of the calculation domain (L) is taken as 0.5 m. Computations are done for different swirl vane angles $\theta = 0^o$, 20^o, 37^o, 56^o, and 66^o corresponding to swirl numbers S = 0, 0.25, 0.50, 1.00 and 1.50, respectively and the results are shown in Figs. 8 – 10. The flow parameters are non-dimensionalized by the reference velocity $U_o = U_1 = 15.6$ m/s.

The distribution of predicted dimensionless mean axial velocity across the flow for the above swirl vane angles at different sections away from the sudden expansion geometry at inlet is shown in Fig. 8 for comparison. Here, one finds that for non-swirling flow ($\theta = 0^o$), one may have small primary recirculation due to sudden expansion as can be seen by the negative *u* velocity near the centerline at x/R = 0.2, similar to Case – I. As the swirl vane angle increases to $\theta = 20^o$, the primary recirculation disappears. But for high swirl ($\theta = 56^o$ and 66^o) large secondary on-axis recirculation due to swirl appears, and increases with the increase of swirl strength. As the inlet axial velocity of the non-swirling cooling air for Case – II is only $U_2 = 7.7$ m/s, compared to 15.4 m/s for Case – I, and the inlet axial velocity of the swirling jet $U_1 = 15.6$ m/s for both cases, so a large drop of the axial velocity is observed near r/R = 0.7.

The variation of the dimensionless mean tangential velocity profiles across the flow at different sections are shown in Fig. 9. At x/R = 0.6, for vane angles $\theta = 56^o$ and 66^o the tangential velocity near the combustor wall has positive value which means that part of the cooling air jet has also started rotating, unlike to that for Case – I in Fig. 5. At $x/R \geq 1.0$, the cooling air jet rotates along with the core swirling flow, for high swirl vane angles. As a result, for high swirl strengths, the rotational shear strain between the core jet and outer cooling air jet and hence the generation of turbulence kinetic energy for Case – II will be lower than that for Case – I. For vane angle $\theta = 20^o$ or 37^o the tangential velocities are not sufficient to make significant difference. Also, as the cooling air starts to rotate with the core flow, it means that the non-swirling cooling air jet for Case – II is not maintaining a proper buffer zone to protect the combustor wall, unlike Case – I in Fig. 5.

Figure 10 shows the variation of the dimensionless turbulence kinetic energy at different axial locations. Here, one observes that with the increase of swirl vane angle the turbulence kinetic energy increases. But, as the rotational shear strain between the inner swirling jet and outer cooling air jet is lower for Case – II than that for Case – I, hence Case – II has lower turbulence kinetic energy generation. At x/R = 0.2, the turbulence kinetic energy generated due to interaction of the two jets near r/R = 0.75 is much lower for Case – II compared to that for Case – I, as can be seen from Fig. 10 and Fig. 6. Consequently, the turbulence kinetic energy found in the later sections for Case – II are also lower.

CONCLUSION

Based on the computational results, the following conclusions may be drawn:

The present computational model is capable of predicting the flow in the combustor with reasonable accuracy.

Moderate or high swirls produce secondary on-axis recirculation which increases with swirl strength.

Swirl produces larger turbulence kinetic energy and enhances the desired mixing rate for complete combustion in a shorter combustor length.

The cooling air admitted close to the combustor wall allows the combustion to occur at a higher temperature while protecting the wall from burnout. It also increases the generation of turbulence kinetic energy for better mixing and complete combustion.

Adequate axial velocity of the non-swirling cooling air jet is needed to properly protect the combustor wall from burnout.

REFERENCES

1. Gerstein, M. (ed), 'Fundamentals of Gas Turbine Combustion', NASA-CP2087, NASA Lewis Research Center, Cleveland, Ohio (1979).
2. Lefebvre, A.H. (ed), 'Gas Turbine Combustor Design Problems', Hemisphere McGraw-Hill, New York (1980).
3. Launder, B.E. and Spalding, D.B., 'The Numerical Computation of Turbulent Flows', Computer Methods in Applied Mechanics and Engineering, Vol. 3, pp.269-289 (1974).
4. Patankar, S.V., 'Numerical Heat and Fluid Flow', McGraw-Hill, New York (1980).
5. Gosman, A.D. and Pun, W.M., 'Calculation of Recirculating Flows', Rept. No. HTS/74/12, Dept. of Mechanical Engineering, Imperial College, London (1974).
6. Brum, and Samuelsen, 'Aerothermal Modeling Program Phase I Final Report', NASA CR-168243, NASA-Lewis Research Center, Cleveland, Ohio (1983).
7. Hogg, S. and Leschziner, M.A., 'Computation of Highly Swirling Confined Flow with a Reynolds Stress Turbulence Model', AIAA Journal, Vol.27, No.1, pp. 57-63 (1989).
8. Chowdhury, S.J. and Anwar, K.O., 'Numerical Analysis of Coaxial Swirling Turbulent Jets with Sudden Expansion', Journal of the Institution of Engineers, India, Vol. 81, pp. 135-140 (2001).